Thermally Responsive Swelling Properties of Polyacrylamide/ Poly(acrylic acid) Interpenetrating Polymer Network Nanoparticles

Donald E. Owens III,[†] Yicun Jian,[‡] Justin E. Fang,[‡] Brandon V. Slaughter,[‡] Yi-Hsuan Chen,[†] and Nicholas A. Peppas*[,†,‡,§]

Departments of Chemical Engineering, Biomedical Engineering, and Pharmaceutics, University of Texas at Austin, 1 University Station, C0400, Austin, Texas 78712

Received May 14, 2007; Revised Manuscript Received July 15, 2007

ABSTRACT: Interpenetrating polymer network (IPN), random copolymer, and homopolymer nanoparticles of acrylamide and acrylic acid were prepared using an inverse emulsion polymerization technique. Differential scanning calorimetry and Fourier-transform infrared spectroscopy were used to examine the molecular structure of the prepared polymeric nanoparticles. The spherical morphology and size (∼250 nm diameter) of the nanoparticles was confirmed using scanning electron microscopy. Dynamic light scattering was used to determine the monodispersity of the particle size distribution and examine the thermally responsive swelling properties of the polymeric nanoparticle structures. Of the particle systems studied, only the IPN nanoparticles exhibited a unique, rapid sigmoidal swelling transition with temperature. These systems also achieved a much larger relative swelling volume compared to random copolymer and homopolymer particles comprised of acrylamide and acrylic acid. Increased cross-linker density resulted in an overall decrease in the maximum relative swelling volume that was obtained.

Introduction

Stimuli-responsive polymer particles, which are capable of responding to changes in their environment such as pH,[1−3] osmotic strength,[4−6] and/or temperature,[7−10] have received growing attention in recent years for applications in a wide variety of areas, including controlled drug delivery.[11−17] Under certain conditions, these stimuli-responsive polymer networks exist in a collapsed state where diffusion or release of an encapsulated agent is limited or prevented by the small size of openings, or mesh size, ξ, in the polymer that comprises the drug delivery device. However, upon activation or change in a specific environmental factor, these particles swell, thereby increasing their mesh size and allowing for the release of any encapsulated agents.

Recently, considerable attention has been paid to a novel class of thermally responsive polymer hydrogels known as interpenetrating polymer networks (IPNs).[18−22] Within the field of thermally responsive hydrogel polymers, two general types exist: those which exhibit a negative or inverse swelling response, which collapse on heating such as poly(*N*-isopropylacrylamide) particles,[23] and those which exhibit a positive swelling response and expand in response to increase in temperature, such as poly(acrylic acid) particles. A further subcategory of positively responsive polymer nanoparticles are those that exhibit a sharp sigmoidal volume transition over a very narrow temperature range usually related to the polymer's upper critical solution temperature (UCST). Interpenetrating polymer network nanoparticles comprised of poly(acrylic acid) (PAA) and polyacrylamide (PAAm) are one of the few systems that exhibit this unique UCST-like behavior.

IPNs are comprised of two or more polymer networks that are not chemically cross-linked with one another, but are interpenetrating or physically entangled within one another such that they cannot be separated. These systems are typically prepared using a sequential IPN synthesis method where one network, in this case the polyacrylamide network, is reacted to completion in the absence of the second network. This fully formed network is then swollen in, or impregnated with, the precursor materials used to form the second polymer network, in this case poly(acrylic acid), thus ensuring the interpenetration and physical entanglement of the two networks upon polymerization of the second network.

The UCST-like swelling behavior of PAA/PAAm IPN nanoparticles is due to their unique structure and the presence of secondary hydrogen-bonding complexes that develop between the PAA and PAAm networks. At lower temperatures hydrogen bonding forces dominate and maintain the particles in a collapsed state; however, as temperature is increased these bonds are weakened and a hydrophilic front is established within the polymer.[24] These two effects work synergistically together to rapidly swell the particles resulting in the UCST-like behavior that is seen in these materials.

The aim of the present work was to synthesize monodisperse interpenetrating polymer network, random copolymer, and homopolymer nanoparticles from polyacrylamide and poly(acrylic acid) and characterize the morphological, structural, and thermally responsive swelling properties of these materials. The effect of cross-linker concentration on the thermally responsive properties of the IPN nanoparticles was also examined.

Experimental Section

Materials. Acrylic acid (AA, inhibited with 200 ppm hydroquinone monomethyl ether), *N*,*N*′-methylenebis(acrylamide) (MBAAm), poly(ethylene glycol) lauryl ether (Brij 30), cyclohexane, and sodium bis(2-ethylhexyl) sulfosuccinate (AOT) were obtained from Sigma Aldrich (Milwaukee, WI), and acrylamide (AAm) and ammonium persulfate (APS) were obtained from Fisher Scientific (Hampton, NH). All materials were used as received.

Synthesis of Polymeric Nanoparticles. PAAm/PAA IPN polymer nanoparticles were synthesized using a two-stage sequential

* Corresponding author. Telephone: 1-(512)-471-6644. Fax: 1-(512)-471-8227. E-mail: peppas@che.utexas.edu.
† Department of Chemical Engineering, University of Texas at Austin.
‡ Department of Biomedical Engineering, University of Texas at Austin.
§ Department of Pharmaceutics, University of Texas at Austin.

10.1021/ma071089x CCC: $37.00
Published on Web 08/29/2007

inverse emulsion polymerization method described previously in the literature.[25−27] The inverse emulsion solution consisted of an 81 wt % cyclohexane continuous phase, with a 13 wt % surfactant phase (AOT and Brij 30 in a 2:1 ratio), and a 6 wt % aqueous phase. The exact composition of the aqueous phase was varied depending on the type of monomer system used and the desired final polymer structure. However, a representative aqueous phase consisted of approximately 11.7 wt % monomer, 2 wt % cross-linker, 5.3 wt % initiator, and 81 wt % water.

In a typical experiment, a three-neck round-bottom flask equipped with a condenser, nitrogen purge line, and overhead mechanical stirrer was first charged with the entire volume of cyclohexane to be used in the polymerization. To this was added the entire emulsifier phase, which dissolved under vigorous stirring. For the first stage of the sequential IPN polymerization, half of the total aqueous phase was added, containing only the acrylamide monomer along with cross-linker, initiator, and deionized distilled water (ddH_2O). This mixture was then purged with nitrogen gas for 30 min to remove oxygen and homogenized (Ultra-Turrax T25, IKA, Wilmington, NC) at 24 000 rpm for 5 min.

After homogenization the polymerization was then initiated thermally by immersion of the reaction vessel in a 60 °C bath and allowed to react to completion (typically 2 h). Upon completion of the first stage of the IPN synthesis, the second stage was then started by adding the other half of the aqueous phase, consisting of additional cross-linker, initiator, and acrylic acid monomer, to the same three-neck round-bottom flask as before. The vessel was again purged with nitrogen gas, homogenized, and allowed to react at 60 °C for 2 h, thus resulting in the formation of the final PAAm/PAA IPN nanoparticles.

PAAm and PAA cross-linked homopolymer nanoparticles and P(AAm-*co*-AA) cross-linked copolymer nanoparticles were also made using the same inverse emulsion polymerization system as the IPN particles except that the aqueous phases were combined and added in a single step. In the case of the copolymer nanoparticles, both AAm and AA monomers were polymerized together in one step. In the case of the homopolymer nanoparticles, both phases were again combined, but only contained AAm monomer in the case of PAAm homopolymer nanoparticles and AA monomer in the case of the PAA nanoparticles.

All of the various polymer batches were then collected and purified by removal of the cyclohexane phase with elevated temperature and reduced pressure (40 °C/50 mmHg) in a rotary evaporator (RE-121, Buchi, Flawil, Switzerland). This was followed by precipitation of the particles out of the emulsifier phase with the addition of excess ethanol and subsequent pelting and washing (three times) by centrifugation (Centra CL3R, Thermo IEC, Waltham, MA) at 3200 rcf. for 60 min. The purified polymer pellet was then resuspended in deionized water in preparation for dialysis cleaning.

All prepared polymeric materials were then placed in dialysis bags (molecular weight cutoff = 14 000 Da) and washed in a ddH_2O reservoir replenished twice daily for 5 days to remove any unreacted materials. The washed polymeric materials were next frozen overnight, then lyophilized, and finally examined in dried powder form or resuspended in the appropriate buffer for further analysis.

Characterization of Polymeric Nanoparticles. The percentage conversions of the various monomers examined in this work were determined using a differential scanning calorimeter (DSC 7, Perkin-Elmer, Wellesley, MA). To obtain these data, batches were prepared using the standard method described above; however, before initiating the polymerization, 60 μL of solution was transferred from the three-neck round-bottom flask to a large volume (60 μL) hermitically sealed DSC pan under an inert atmosphere. The pan was weighed before and after addition of the sample using a high accuracy analytical balance to determine the exact weight of the added sample. Then an isothermal DSC characterization method, described below, was used to measure the total heat evolved during polymerization.

The hermitically sealed DSC samples were heated from 25 to 60 °C at a rate of 100 °C/min and held at 60 °C for 3 h, during which time the thermal energy evolved by the polymerization was measured and recorded. After 3 h the sample was then heated to 120 °C at a rate of 10 °C/min and held for 15 min and then cooled at a rate of 10 °C/min back to 25 °C. This same ramp was then applied a second time, to establish a baseline heating profile, and the difference in thermal energy evolved between these last two ramps was used as a measure of the unreacted monomer present in the system. Finally, the experimentally measured total energy evolved was also compared to the theoretical total energy available based on the weight of monomer added to the DSC pan and heat of polymerization values found in the literature for the various monomers that were polymerized. Each monomer was run in triplicate to ensure the reproducibility of the calculated percentage conversion.

Table 1. DSC Analysis of the Experimental and Theoretical Conversion of the Various Monomer Systems Utilized in This Work

monomer	polymer structure	experimental conversion (%)	theoretical conversion (%)
AAm only	linear	96.92 ± 1.13	96.15 ± 0.25
AA only	linear	85.72 ± 0.83	87.48 ± 4.20
AAm + cross-linker	nanoparticle	94.52 ± 0.45	92.25 ± 0.71
AA + cross-linker	nanoparticle	81.36 ± 0.38	79.19 ± 2.66

Table 2. DSC Analysis of the Experimental and Theoretical Conversion of the Various Monomer Systems Utilized in This Work

polymer system	molar feed ratio (%)		final IPN molar ratio (%)		cross-linker (mol %)	max RSV RSV ± STD
	AAm	AA	AAm	AA		
PAAm	100	0	100	0	0.1	1.13 ± 0.04
PAA	0	100	0	100	0.1	13.00 ± 1.99
P(AAm-*co*-AA)	46	54	50	50	0.1	35.22 ± 2.55
PAAm/PAA IPN	46	54	50	50	0.1	86.85 ± 8.23
PAAm/PAA IPN	46	54	50	50	0.25	32.35 ± 1.48
PAAm/PAA IPN	46	54	50	50	0.5	12.14 ± 1.24
PAAm/PAA IPN	46	54	50	50	1	1.85 ± 0.11
PAAm/PAA IPN	46	54	50	50	10	1.12 ± 0.10

The infrared spectra of the polymeric nanoparticles was obtained in the wavenumber range of 400−4000 cm^{-1} using a Fourier transform infrared spectrophotometer (FT-IR, Thermo Mattson Infinity, Thermo Electron Corp., Waltham, MA) in transmission mode equipped with a KBr beamsplitter and DTGS detector. To obtain this data, 1 mg of lyophilized polymeric material in powder form was thoroughly mixed with 150 mg of KBr and pressed into a pellet for analysis using a Carver laboratory press operating at 15 000 lbs of compressive force for 5 min.

The morphology of the polymeric nanoparticles was examined using a field emission scanning electron microscope (FE-SEM, 1530, LEO, Oberkochen, Germany) operating at 10 kV. Purified samples were first frozen overnight and then lyophilized in a 4.5 liter manifold lyophilizer (Freezone, Labconco, Kansas City, MI). To prepare the samples for imaging, the polymeric nanoparticles in powder form were then mounted on an aluminum SEM stage and coated with gold for 30 s using a sputter-coater (model 3, Pelco, Redding, CA) in an inert argon atmosphere.

The hydrodynamic diameter of the particles in solution as a function of temperature and the particle size distribution was determined using a dynamic light scattering (DLS, ZetaPlus, Brookhaven, Holtsville, NY) instrument operating at a 90° scattering angle with a 635 nm, 35 mW diode laser source. To obtain this data, washed and dried particles were resuspended in an aqueous buffer and their hydrodynamic diameter was measured in 2 °C increments from 25 to 55 °C.

Results and Discussion

Nanoparticle Composition and Morphology. It has been previously shown[24] that the ratio of acrylamide to acrylic acid repeat units in the final IPN structure is critical to achieving enhanced thermally responsive properties. Specifically, the

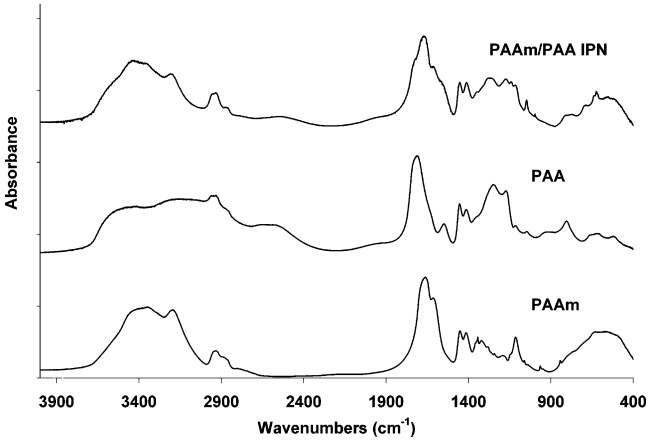

Figure 1. FT-IR absorption spectra of polyacrylamide (PAAm), poly(acrylic acid) (PAA), and PAAm/PAA interpenetrating polymer network nanoparticles.

ability to obtain a sharp transition with temperature as well as a large volume change from the collapsed to swollen state is decreased as the final IPN structure moves further away from the ideal situation of a 1:1 molar ratio of repeat units.[28,29] Therefore, it was critical to know the exact conversion rate of the various monomers in this specific emulsion system so that feed ratios could be selected to ensure a 1:1 monomer ratio in the final IPN structure.

In order to ensure that this requirement was met, the various monomers were analyzed individually, both with and without added cross-linker, using differential scanning calorimetry to determine their overall percentage conversion within the inverse emulsion polymerization system. Samples were run in triplicate and the average of all runs ± one standard deviation is summarized in Table 1. Theoretical conversions were calculated using the mass of added monomer in a given experiment and the heat of polymerization values: 81.5 kJ/mol for AAm,[30] 77.5 kJ/mol for AA,[31] and 82.7 kJ/mol for MBAAm.[32] From Table 1, it is apparent that the first step of the IPN synthesis reaction involving the formation of the polyacrylamide portion of the network goes nearly to completion as evidenced by the high experimental percentage conversion of 94.52 ± 0.45. Furthermore, the addition of cross-linker does not appear to have a major impact on the overall percentage conversion of the various monomers. These conversion results were then used to determine the feed ratios of the various monomers necessary to ensure a 1:1 ratio of acrylamide and acrylic acid repeat units in the final IPN structure. The results of this analysis are listed in Table 2.

The molecular structure of the IPN nanoparticles was further investigated using FT-IR. Figure 1 shows the combined FT-IR spectra of homopolymer nanoparticles of PAAm and PAA, and PAAm/PAA IPN nanoparticles. In Figure 1 a mixture of absorption bands from both the PAAm and PAA portions of PAAm/PAA IPN nanoparticles was evident. A broad and shifted C═O band at 1680 cm^{-1} was due to the combined stretching vibrations of the C═O groups of both PAAm (1665 cm^{-1}) and PAA (1720 cm^{-1}) as well as the effects of hydrogen bonding present in the IPN structure.[33] Absorption bands at 1455 and 1416 cm^{-1} were due to the scissor and bending vibrations of CH_2 and CH−CO groups, respectively. Furthermore, the absorption band at 2950 cm^{-1} corresponded to the combined stretching of CH_2 groups in both the PAAm (2945 cm^{-1}) and PAA (2960 cm^{-1}) portions of the IPN structure. Finally, the broad absorption bands in the 3100 to 3500 cm^{-1} regions were due to the overlapping absorption bands of O−H and NH_2 stretching vibrations, while the absorption bands in the 1150 to 1300 cm^{-1} region were due to the overlap of the stretching C−N, and C═O coupled with the bending of O−H groups.[33]

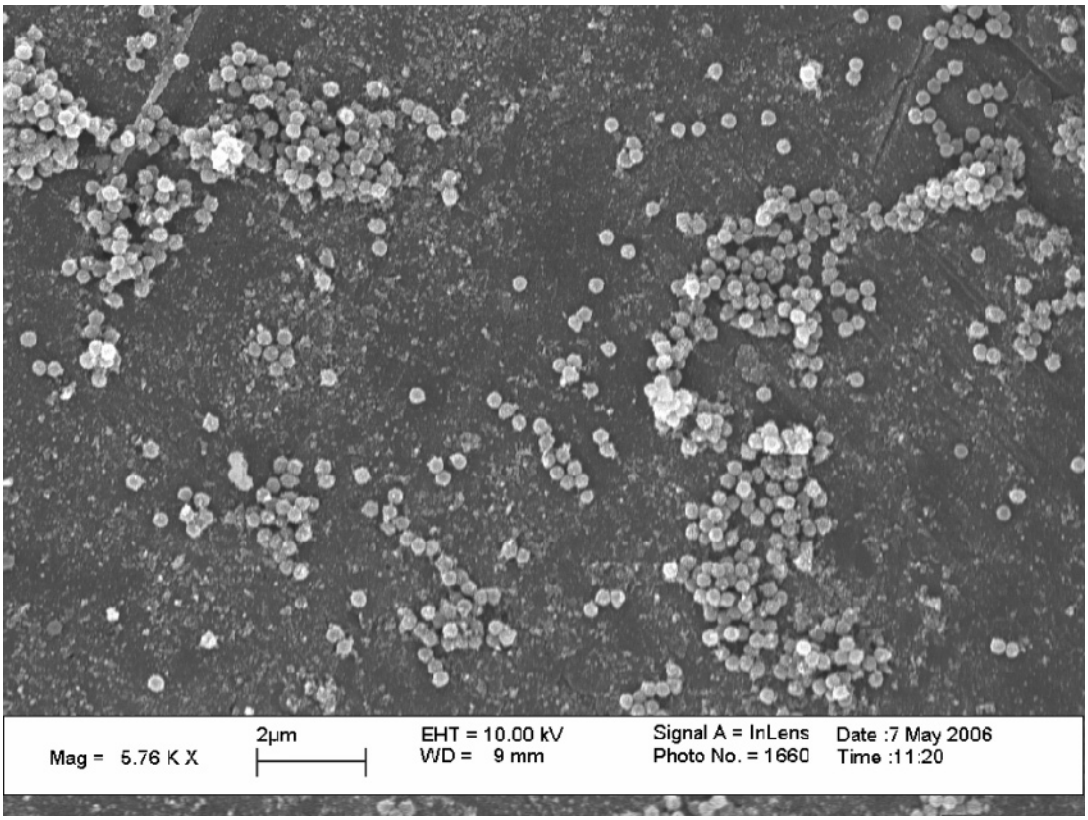

Figure 2. Representative low magnification SEM micrograph of polymeric nanoparticles prepared by an inverse microemulsion polymerization and subsequent dialysis and lyophilization technique.

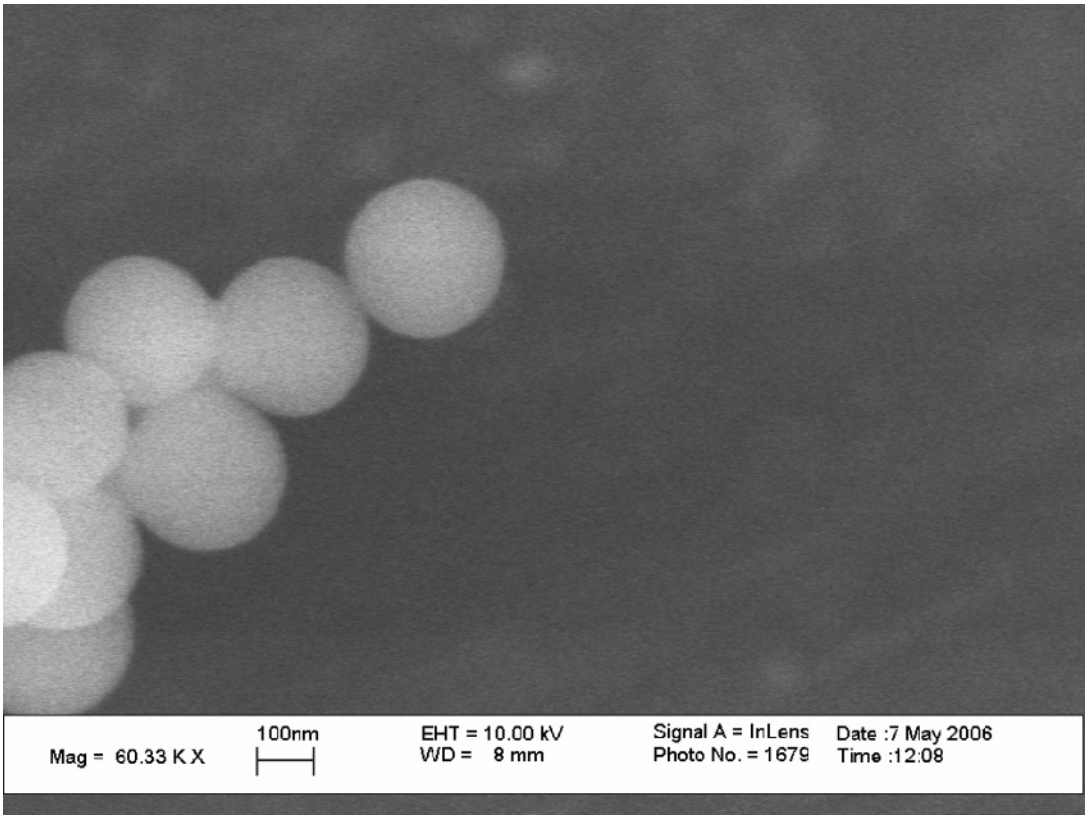

Figure 3. Representative high magnification SEM micrograph of polymeric nanoparticles prepared by an inverse microemulsion polymerization and subsequent dialysis and lyophilization technique.

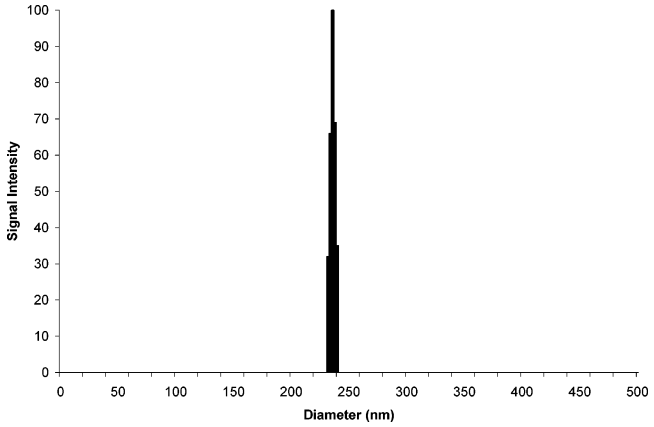

Figure 4. Representative dynamic light scattering analysis of the distribution of hydrodynamic diameters present in a sample of polymeric nanoparticles prepared by an inverse microemulsion polymerization after dialysis, lyophilization, and subsequent resuspension.

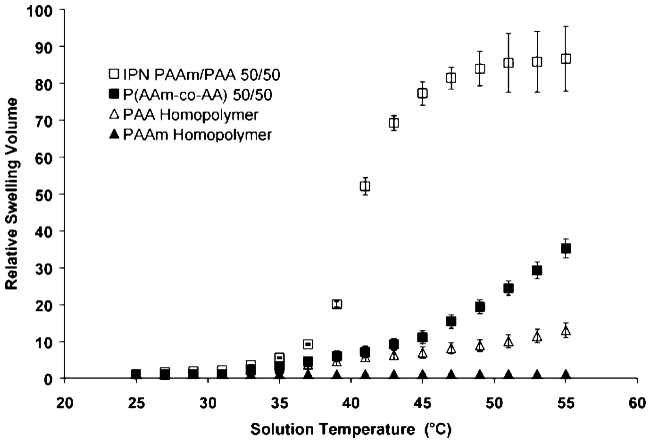

Figure 5. Dynamic light scattering study of the thermally responsive swelling behavior of polymeric nanoparticles comprised of both polyacrylamide and poly(acrylic acid) homopolymers, a random copolymer of poly(acrylamide-*co*-acrylic acid), and a polyacrylamide/poly(acrylic acid) IPN, suspended in a pH 3 aqueous buffer.

Scanning electron microscopy was utilized to examine the morphology of the particles as shown in the representative low and high magnification micrographs of lyophilized PAAm/PAA IPN nanoparticles, Figures 2 and 3, respectively. The particles also appeared to be monodisperse in size with an average diameter of approximately 240 nm as confirmed by dynamic light scattering analysis of the particles in solution (Figure 4).

Swelling Studies. Dynamic light scattering was used to examine the effect of polymeric structure on the swelling properties of various polyacrylamide and poly(acrylic acid) nanoparticles suspended in a pH 3 aqueous buffer. In this study homopolymer nanoparticles of both polyacrylamide and poly(acrylic acid) were compared to a random copolymer of poly(acrylamide-*co*-acrylic acid) as well as polyacrylamide/poly(acrylic acid) IPN nanoparticles. Figure 5 shows the change in relative swelling volume (RSV) for each of the various polymeric nanoparticle systems. For the purposes of this research, the relative swelling volume (RSV) is defined as the average volume of the swollen particles at a specified temperature over the average volume of the collapsed particles, where the collapsed volume is simply the average volume of particles in solution at 25 °C as determine by dynamic light scattering measurement. From this graph, it is clear that the IPN polymer structure yielded a much large maximum RSV as well as a sharper UCST-like swelling transition. The random copolymer, as well as the poly(acrylic acid) homopolymer, exhibited some swelling with temperature and the homopolymer polyacrylamide particle exhibited almost no swelling with increased temperature. Error bars in the graph represent one standard deviation, $n =$

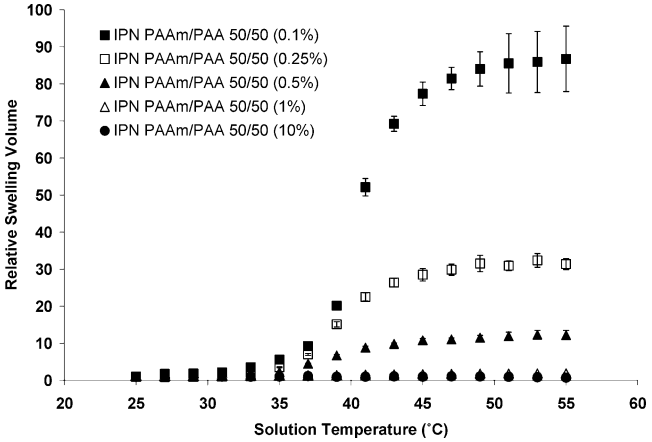

Figure 6. Effect of cross-linker concentration on the thermally responsive swelling properties of a series IPN nanoparticle samples, suspended in an aqueous pH 3 buffer solution.

10, and generally tended to increase as the diameter of the particles increased. This trend was due to an overall decrease in the optical density and scattering efficiency of hydrogel particles in the swollen state, which leaded to higher variability in the measured hydrodynamic diameter. The monomer ratios and molar percentages of cross-linker used to prepare these polymer nanoparticles, as well as the maximum RSV achieved, are listed in Table 2.

The effect of cross-linking density on the thermally responsive swelling properties of a series IPN nanoparticle samples, suspended in an aqueous pH 3 buffer solution, is clearly illustrated in Figure 6. The monomer ratios and cross-linker density used to prepare these IPN nanoparticles, as well as the maximum RSV achieved, are listed in Table 2. All the IPN particles described in this table were synthesized with an initiator concentration of 7 wt % with respect to the total mass of monomer and cross-linker. From this graph it is clear that increased cross-linking density led to a decrease in the final volume swelling ratio of the IPN particles.

Conclusions

Thermally responsive polymeric nanoparticles comprised of polyacrylamide and poly(acrylic acid) were successfully synthesized using an inverse microemulsion polymerization technique. Scanning electron microscopy was used to confirm that the particles had a spherical morphology with an average size in the biologically relevant region of 300 nm diameter and below. Dynamic light scattering (DLS) studies further confirmed the monodisperse size distribution of polymeric nanoparticles prepared using this technique.

Differential scanning calorimetric studies were conducted to determine the percentage conversion obtained by each monomer system polymerized in the inverse microemulsion environment. The results of these studies were then used to formulate interpenetrating polymer networks (IPNs) and random copolymers in such a way that the final polymer structures would contain a 1:1 ratio of acrylamide to acrylic acid repeat units. Fourier transfer infrared analysis was used to further confirm the presence of functional groups from both PAAm and PAA in the final PAAm/PAA IPN nanoparticles.

DLS studies were also used to confirm the unique upper critical solution temperature behavior of the IPN nanoparticles and the increased maximum relative swelling volume obtained by this polymer structure compared to random copolymer and homopolymer structures of similar size and composition. The dependence of the maximum relative swelling volume on cross-linker density, for the IPN nanoparticle systems, was also elucidated.

Acknowledgment. This work was supported in part by a grant from the National Science Foundation, CTS-03-29317 and by a National Science Foundation Integrative Graduate Education and Research Traineeship (IGERT) Fellowship (to D.E.O.III), DGE-03-33080.

References and Notes

(1) Thomas, J. B.; Creecy, C. M.; McGinity, J. W.; Peppas, N. A. *Polym. Bull. (Berlin)* **2006**, *57*, 11−20.
(2) Morishita, M.; Goto, M.; Takayama, K.; Peppas, N. A. *J. Drug Deliv. Sci. Technol.* **2006**, *16*, 19−24.
(3) Oral, E.; Peppas, N. A. *J. Biomed. Mater. Res.* **2004**, *68A*, 439−447.
(4) Khare, A. R.; Peppas, N. A. *Biomaterials* **1995**, *16*, 559−567.
(5) Catellani, P. L.; Colombo, P.; Peppas, N. A.; Santi, P.; Bettini, R. *J. Pharm. Sci.* **1998**, *87*, 726−731.
(6) Brunner, A.; Mader, K.; Gopferich, A. *Pharm. Res.* **1999**, *16*, 847−853.
(7) Bromberg, L. E.; Ron, E. S. *Adv. Drug Deliv. Rev.* **1998**, *31*, 197−221.
(8) Zhang, J.; Peppas, N. A. *J. Biomater. Sci., Polym. Ed.* **2002**, *13*, 511−525.
(9) Vakkalanka, S. K.; Brazel, C. S.; Peppas, N. A. *J. Biomater. Sci., Polym. Ed.* **1996**, *8*, 119−129.
(10) Brazel, C. S.; Peppas, N. A. *J. Controlled Release* **1996**, *39*, 57−64.
(11) Jeong, B.; Kim, S. W.; Bae, Y. H. *Adv. Drug Deliv. Rev.* **2002**, *54*, 37−51.
(12) Kim, S. W.; Bae, Y. H.; Okano, T. *Pharm. Res.* **1992**, *9*, 283−290.
(13) Qiu, Y.; Park, K. *Adv. Drug Deliv. Rev.* **2001**, *53*, 321−339.
(14) Langer, R.; Peppas, N. A. *AIChE J.* **2003**, *49*, 2990−3006.
(15) Byrne, M. E.; Park, K.; Peppas, N. A. *Adv. Drug Deliv. Rev.* **2002**, *54*, 149−161.
(16) Kim, B.; Peppas, N. A. *Int. J. Pharm.* **2003**, *266*, 29−37.
(17) Peppas, N. A.; Leobandung, W. *J. Biomater. Sci., Polym. Ed.* **2004**, *15*, 125−144.
(18) Liu, Y. Y.; Lu, J.; Shao, Y. H. *Macromol. Biosci.* **2006**, *6*, 452−458.
(19) Shi, J.; Alves, N. M.; Mano, J. E. *Macromol. Biosci.* **2006**, *6*, 358−363.
(20) Wu, W.; Li, W. J.; Wang, L. Q.; Tu, K. H.; Sun, W. L. *Polym. Int.* **2006**, *55*, 513−519.
(21) Guilherme, M. R.; Campese, G. M.; Radovanovic, E.; Rubira, A. F.; Tambourgi, E. B.; Muniz, E. C. *J. Membr. Sci.* **2006**, *275*, 187−194.
(22) Xiao, X. C.; Zhuo, R. X.; Xu, J.; Chen, L. G. *Eur. Polym. J.* **2006**, *42*, 473−478.
(23) Pelton, R. *Adv. Colloid Interface Sci.* **2000**, *85*, 1−33.
(24) Okano, T. *Adv. Polym. Sci.* **1993**, *110*, 179−197.
(25) Daubresse, C.; Grandfils, C.; Jerome, R.; Teyssie, P. *Colloid Polym. Sci.* **1996**, *274*, 482−489.
(26) Daubresse, C.; Grandfils, C.; Jerome, R.; Teyssie, P. *J. Colloid Interface Sci.* **1994**, *168*, 222−229.
(27) Bouillot, P.; Vincent, B. *Colloid Polym. Sci.* **2000**, *278*, 74−79.
(28) Katono, H.; Maruyama, A.; Sanui, K.; Ogata, N.; Okano, T.; Sakurai, Y. *J. Controlled Release* **1991**, *16*, 215−227.
(29) Aoki, T.; Kawashima, M.; Katono, H.; Sanui, K.; Ogata, N.; Okano, T.; Sakurai, Y. *Macromolecules* **1994**, *27*, 947−952.
(30) Joshi, R. M. *J. Polym. Sci.* **1962**, *56*, 313−338.
(31) McCurdy, K. G.; Laidler, K. J. *Can. J. Chem.* **1964**, *42*, 818−824.
(32) Verneker, V. R. P.; Santhanalakshmi, K. N. *J. Polym. Sci. Pol. Chem.* **1984**, *22*, 3217−3224.
(33) Moharram, M. A.; Balloomal, L. S.; El Gendy, H. M. *J. Appl. Polym. Sci.* **1996**, *59*, 987−990.

MA071089X